

# Challenge-Response to Authenticate Drone Communications: A Game Theoretic Approach

Mattia Piana, *Student Member, IEEE*, Francesco Ardizzon, *Member, IEEE*, and Stefano Tomasin, *Senior Member, IEEE*

**Abstract**—In this paper, we propose a novel strategy for physical layer authentications based on the challenge-response concept for a transmitting drone (Alice). In a preliminary training phase, Alice moves over several positions, and Bob (either a drone or a ground device) estimates the Alice-Bob channel gains. Then Alice transmits its message from different random positions (challenge) and Bob, upon receiving the messages, authenticates the sender via a log-likelihood test on the estimated channel gains (response). In turn, the intruder Trudy selects random positions on which she transmits messages on behalf of Alice to Bob. In this paper, we design the probability mass distribution of Alice’s challenge positions and the Trudy response positions by modeling the problem as a zero-sum game between Bob and Trudy, where the payoff of Trudy is the missed detection probability. Moreover, we propose three different approaches that minimize the energy spent by Alice without sacrificing security, which differ in computational complexity and resulting energy consumption. Finally, we test the proposed technique via numerical simulations, which include a realistic model of both Alice-Bob and Trudy-Bob fading channels, affected by shadowing.

**Index Terms**—Authentication, Challenge-and-response, Drone communications, Game Theory, Physical layer security, Unmanned Aerial Vehicles.

## I. INTRODUCTION

The use of drones has rapidly increased over the last few years. Starting as a military tool, they are now used in many civil applications such as precision agriculture, environmental monitoring, and disaster management and relief. As drones become integrated into more complex systems, security is a rising concern [1], and among major threats, the transmission of jamming or spoofing signals is particularly dangerous since they can disrupt the navigation system [2], [3] and jeopardize the drone mission.

This paper addresses the problem of authentication of messages transmitted by drones. In particular, a drone or a ground device (Bob) aims to authenticate messages potentially transmitted by a legitimate drone (Alice), distinguishing them from those transmitted by an *intruder* drone (Trudy), who aims to impersonate Alice. Cryptography-based solutions for such

authentication problems have several issues, as a) they are computationally expensive, b) they provide only computational security, that may be beaten with quantum computing, and c) they have a significant communication overhead to contact trusted nodes and renew secret keys used to encrypt messages. Both communication overhead and computational complexity lead to high consumption of energy, a limited resource for drones. Hence, in this paper, we focus on physical layer authentication (PLA) mechanisms that provide security based on the statistical properties of the Alice-Bob channels. These techniques typically require less energy than their crypto-based counterparts while still providing information-theoretic security.

PLA has been recently surveyed in [4], [5] and mechanisms specifically targeting drone communications may rely on fingerprinting [6], or on the channel characteristics, eventually aided by a federated learning architecture [7]. Here we focus on a recent advancement of PLA, using a challenge-response (CR) approach. In cryptographic-based CR authentication [8, Sec. 13.5], Alice and Bob share a secret key. Then, Bob transmits over a public channel a message, called *challenge*, and Alice computes and transmits back to Bob a *response* obtained using a hash function of both the secret key and the challenge. Lastly, Bob verifies the authenticity of the response’s sender by matching the response and a local response, obtained using the same secret key and challenge. Instead of relying on crypto-based solutions, we consider PLA-based CR, first introduced in [9]. CR-PLA is based on *partially controllable channels* where the challenge is issued by the verifier Bob through manipulation of the propagation environment, while the response is the received signal from Alice, which must be consistent with the expected change. As the challenge, i.e., the propagation conditions, is randomly decided by the verifier, it is difficult for Trudy to predict it and transmit a signal that is consistent with it.

In [10] and [11] the authors proposed a first CR-PLA protocol for drone communications. However, a simple channel model was considered and the challenge distribution was not optimized but chosen as uniform; also the attacks were not optimized. In this work, instead, we consider a more complete channel model and exploit its characteristics, particularly shadowing, to design the challenge distribution and investigate more sophisticated attacks.

Aside from our previous work [11], while there are studies on the energy consumption of drones, e.g., [12], only a few studies analyze the link between energy consumption and physical layer security protocols. The analyses typically target

Manuscript received –; revised – and – accepted –. Date of publication –; date of current version –.

Corresponding author: M. Piana. This work was partially supported by the European Union under the Italian National Recovery and Resilience Plan (PNRR) of NextGenerationEU, partnerships on “Telecommunications of the Future” (PE0000001 - program “RESTART and PE00000014 - program “SERICS”), and through the Horizon Europe/JU SNS project ROBUST-6G (Grant Agreement no. 101139068). The authors are with the Department of Information Engineering, Università degli Studi di Padova, Padua 35131, Italy. S. Tomasin is also with the National Inter-University Consortium for Telecommunications (CNIT), 43124 Parma, Italy. (email: {mattia.piana@studenti., francesco.ardizzon@, stefano.tomasin@}unipd.it).

the energy consumption of crypto/higher-level solutions, e.g., [13].

In this paper, we propose novel strategies for Bob and Trudy when using CR-PLA in drone communications. In particular, in a preliminary phase, Bob measures the channel gain when Alice is in a set of predefined positions. Then, the authenticated transmission protocol provides that first Bob selects at random (with a suitable distribution) a set of positions and communicates it secretly to Alice. Alice goes to the indicated positions and from each of them she transmits a pilot signal together with the message to be authenticated. Next, Bob assesses the authenticity of the received signal by checking that the measured channel gains correspond to the expected ones, estimated in the preliminary phase. In this context, the challenge is represented by the set of positions and the corresponding response is the set of channel gains estimated by Bob. In turn, for her attack, Trudy selects at random (with a suitable distribution) a set of positions from which she transmits the pilot signal and her message. The distributions used by Bob and Trudy to select the position sets are optimized to their advantage by finding the Nash equilibria (NEs) of a zero-sum game. Additionally, we also consider the problem of energy minimization for the Alice movements, by proposing both optimal and heuristic strategies to minimize the (average) distance traveled by Alice without sacrificing the protocol security.

The contributions of this paper are as follows

- We model the drone-to-receiver channel, considering both the channel estimation phase and the actual security protocol.
- We design the statistical distribution of the positions generated by Bob and Trudy by modeling the problem as a zero-sum game between legitimate users and Trudy, where the payoff is the missed detection (MD) for a target false alarm (FA).
- Both optimal and low-complexity solutions for the optimization of the position selection statistics at Bob are considered.
- We test the proposed technique via numerical simulation, based on a realistic model of both Alice-Bob and Trudy-Bob channels, including also shadowing effects.

Several works showed the effectiveness of game theory in authentication. In [14] the authors use game theory to design an authentication protocol for multiple-input and multiple-output (MIMO) channels. A game theoretic authentication protocol for fifth-generation (5G) Internet of Things (IoT) zero-trust networks is proposed in [15]. The multi-agent scenario where multiple receivers and spoofers play has been analyzed in [16].

A game theoretic PLA protocol for drone communication was proposed in [17], where Bob chooses the detection thresholds while Trudy plays by choosing the attack probability. Still, they consider a more restrictive model, where the test is performed by assuming that the previously received signal was authentic, and thus, the signal under test should be matched to the previous.

The rest of the paper is organized as follows. Section II details the system model. Section III gives an overview of the

proposed protocol. The problem of CR-PLA is further characterized in Section IV, while Section V details its solution using game theory. Numerical results are reported in Section VI. Section VII draws the conclusion.

## II. SYSTEM MODEL

In the considered scenario, Alice is a legitimate drone transmitting messages to Bob, which can be a ground device or, eventually, a second drone. A third drone, Trudy, is sending fraudulent messages to Bob. Receiver Bob aims to distinguish messages coming from Alice and Trudy. To this end, we exploit Alice's mobility to design a CR-PLA protocol. In turn, Trudy aims to fool Bob by forging her transmissions so that Bob confuses Trudy's messages as legitimate, i.e., as coming from Alice.

Without loss of generality, we use a Cartesian coordinate system, centered on Bob, to describe any device position. Let  $\mathbf{x} = (x_1, x_2, x_3)$  the generic position of Alice and  $\mathbf{y} = (y_1, y_2, y_3)$  the generic position of Trudy. In particular, we consider the space where the Alice and Trudy move to be sampled by a plane grid at altitude  $h$  containing  $M_A$  and  $M_T$  positions respectively. Thus, Alice's positions are the set

$$\mathcal{X} = \{\mathbf{x}(i) = (x_{i,1}, x_{i,2}, h), \quad i = 1, \dots, M_A\}. \quad (1)$$

Trudy instead can move to positions in a plane grid at the same altitude  $h$  of Alice, containing  $M_T \geq M_A$  positions, and therefore  $\mathcal{X} \subseteq \mathcal{Y}$ . Hence, Trudy positions are the set

$$\mathcal{Y} = \{\mathbf{y}(j) = (y_{j,1}, y_{j,2}, h), \quad j = 1, \dots, M_T\}. \quad (2)$$

While considering a finite set of positions (e.g., on a grid) makes the design of the authentication protocol easier, i) the results can be straightforwardly extended to a general 3D model ii) the map can be very dense allowing Alice to go everywhere on the grid, up to the accuracy of the drone positioning system.

Exploiting Alice mobility for authentication purposes also entails an energy cost. The energy consumed by Alice to move from position  $\mathbf{x}(i)$  to  $\mathbf{x}(i')$  traveling on a straight line is denoted as  $E(\mathbf{x}(i), \mathbf{x}(i'))$ . In particular, assuming Alice moves at a constant speed  $v$  on the horizontal plane, the energy consumption (in Joule) is a linear function of the distance [12], namely

$$E(\mathbf{x}(i), \mathbf{x}(i')) = \alpha_1 \frac{d_{i,i'}}{v} - \alpha_0, \quad (3)$$

where  $\alpha_1$  and  $\alpha_0$  are constants parameters and the distance between position  $\mathbf{x}(i)$  and  $\mathbf{x}(i')$  is

$$d_{i,i'} = \|\mathbf{x}(i') - \mathbf{x}(i)\|. \quad (4)$$

Hence, since in (3) the energy is a function of the traveled distance, we will consider the travelled distance instead of the energy as a cost metric.

### A. Channel Model

Communications among devices occur through narrowband additive white Gaussian noise (AWGN) channels, and their attenuations include path loss, shadowing, and fading. Path loss takes into account the average attenuation caused by the

distance traveled by the signal while shadowing accounts for the presence of objects/obstacles in the environment and is a slow-fading phenomenon, i.e., it changes slowly over time.

Let  $A_{\text{Tx}}$  and  $A_{\text{Rx}}$  be the gains of the transmitter and receiver antennas, respectively. Letting  $(f_c)_{\text{MHz}}$  be the carrier frequency in MHz and  $(d)_{\text{km}} = \|\mathbf{q}\|$  the distance (in km) between transmitter in a generic position  $\mathbf{q}$  and the receiver Bob, we define the path-loss attenuation according to the Friis formula (in dB) as

$$(\xi_{\mathbf{q}})_{\text{dB}} = 32.4 + 10\alpha \log_{10} (d)_{\text{km}} + 20 \log_{10} (f_c)_{\text{MHz}} + A_{\text{Tx}} - A_{\text{Rx}}, \quad (5)$$

where  $\alpha > 1$  is a coefficient determined by the propagation medium.

According to the Gudmundson model [18], the shadowing attenuation in dB  $(s)_{\text{dB}}$  follows a zero-mean normal distribution with variance  $\sigma_{(s)_{\text{dB}}}^2$  (in short  $(s)_{\text{dB}} \sim \mathcal{N}(0, \sigma_{(s)_{\text{dB}}}^2)$ ). The shadowing attenuations  $(s)_{\text{dB}}$  and  $(s')_{\text{dB}}$ , measured at positions  $\mathbf{q}$  and  $\mathbf{q}'$ , are correlated: defining  $d_{\text{ref}}$  as the coherence distance [19], the correlation is

$$\mathbb{E}((s)_{\text{dB}}(s')_{\text{dB}}) = \sigma_{(s)_{\text{dB}}}^2 \exp\left(-\frac{\|\mathbf{q} - \mathbf{q}'\|}{d_{\text{ref}}}\right), \quad (6)$$

where  $\mathbb{E}(\cdot)$  defines the expectation operator. Lastly, when the transmitter is in  $\mathbf{q}$ , the total channel attenuation in dB is [19]

$$(a_{\mathbf{q}})_{\text{dB}} = (\xi_{\mathbf{q}})_{\text{dB}} + (s)_{\text{dB}}. \quad (7)$$

From (7), the average channel amplitude (in linear scale) can be written as

$$\tilde{g}_{\mathbf{q}} = 10^{-\frac{(a_{\mathbf{q}})_{\text{dB}}}{20}}. \quad (8)$$

The signal received and sampled by Bob with sampling period  $T_s$  upon transmission of a symbol  $b_k$  at time  $k$  is described as [20, Sec. 2.4.2]

$$r_k = \tilde{g}_{\mathbf{q}} h_k e^{-j\phi} b_k + w_k, \quad (9)$$

where  $\phi$  is the common phase term due to the signal traveled distance,  $h_k \sim \mathcal{CN}(0, 1)$  is a complex Gaussian circularly symmetric random variable due to the (fast) fading, and  $w_k \sim \mathcal{CN}(0, \sigma_w^2)$  is the thermal noise with variance  $\sigma_w^2$ .

We assume that the symbol period is such that the fading coefficients  $h_k$  are i.i.d. random variables. This occurs if  $T_s > T_c$ , where  $T_c$  is the coherence time, i.e., the time period over which the fading term  $h_k$  in (9) can be considered constant. In turn,  $T_c$  depends on the velocity of objects in the surrounding environment: the faster the environment changes, the shorter  $T_c$  is. Given as the maximum speed  $v_{\text{max}}$  of object movement with respect to Bob and  $c$  as the speed of light in the air, the Doppler frequency shift experienced by Bob is

$$f_D = f_c \frac{v_{\text{max}}}{c}, \quad (10)$$

and following the Clarke's model [21], the coherence time is

$$T_c = \sqrt{\frac{9}{16\pi}} \frac{1}{f_D}. \quad (11)$$

## B. Channel Gain Estimation

As detailed in Section III, Bob uses the channel gain as an authentication feature. To this end, Alice transmits  $K$  unit-power phase-shift keying (PSK) pilot symbols  $b_k$ ,  $k = 1, \dots, K$ , with  $|b_k|^2 = 1$ . Since fading and thermal noise are two independent processes, for the transmission of independent unit power symbols, from (9) we have  $r_k \sim \mathcal{CN}(0, \tilde{g}_{\mathbf{q}}^2 + \sigma_w^2)$ .

Bob estimates the average channel gain (which depends on the transmitter position  $\mathbf{q}$ ) upon the reception of a message as

$$\hat{m} = \mu(\mathbf{q}) = \frac{1}{K} \sum_k |r_k b_k^*|^2 = \frac{1}{K} \sum_k |\tilde{g}_{\mathbf{q}} h_k e^{-j\phi} + w'_k|^2, \quad (12)$$

where  $w'_k$  has the same statistics as  $w_k$  as the transmitted symbols have unitary power.

## C. Attacker Knowledge

We consider the worst-case scenario for Bob, where Trudy can arbitrarily move close to Alice. Moreover, Trudy knows:

- 1) the Bob's location,
- 2) the set  $\mathcal{X}$  of possible Alice's positions,
- 3) the pilot sequence  $\{b_k\}$ ,  $k = 1, \dots, K$ , used by Alice to communicate with Bob.

## III. CHALLENGE-RESPONSE PHYSICAL LAYER AUTHENTICATION

We propose a physical layer authentication mechanism where Bob aims to authenticate received messages by testing the channel gains estimated from the pilot signals. Fig. 1 reports the scheme of the proposed CR-PLA protocol.

The sequence of estimated channel gains is compared against the expected sequence, derived by knowing the positions from which Alice transmitted the signal. Using the channel gains to decide the authenticity of the signal, allows Bob to i) avoid using the channel phase, which may lead to errors due to synchronization differences, and ii) mediate over noise and fading realizations to make a more reliable decision.

We now introduce the proposed CR-PLA protocol. The protocol comprises a set-up and an authentication phase.

### Set-up phase:

- 1) *Reference Gains Estimation*: we assume that Alice and Bob can transmit authenticated pilot signals, for instance by using a higher-layer authentication protocol. This is a training phase, typical of the PLA schemes (e.g., [10], [14], [22], [23]), aimed at acquiring information used in our authentication protocol. In particular, Alice moves in all the positions in  $\mathcal{X}$  and transmits authenticated pilot signals to Bob. Then, Bob estimates the channel gain from each Alice's position from (12). We assume this estimate to be perfect, i.e.,  $K \simeq \infty$  in (12). Bob then obtains the *channel gain map*

$$\mathcal{M} = \{m(i), i = 1, \dots, M_A\}. \quad (13)$$

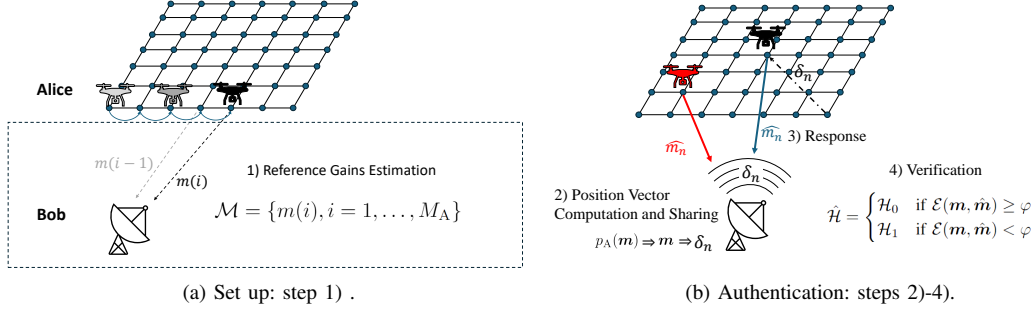


Fig. 1. Scheme of the proposed CR-PLA protocol.

**Authentication phase** (to be repeated for each message transmitted by Alice):

- 2) *Position Vector Computation and Sharing*: Bob randomly draws a vector  $\mathbf{m} = [m_1, \dots, m_N]$ ,  $m_n \in \mathcal{M}$  of  $N$  gains from the gain map, using probability mass distribution (PMD)  $p_A(\mathbf{m})$ . The design of  $p_A(\mathbf{m})$  is discussed in Sections IV and V. Gains are mapped into corresponding positions  $\mathbf{x}_A = [x_1, \dots, x_N]$ , with  $x_n \in \mathcal{X}$ , providing the average gains  $\mathbf{m}$ . Next, Bob communicates the set of positions  $\mathbf{x}_A$  to Alice, without disclosing them to Trudy, as better described in the following. This is considered the *challenge* of the CR protocol.
- 3) *Response*: The transmission of a message by Alice is split into  $N$  rounds, where at each round  $n$  Alice goes to position  $\mathbf{x}_n$  and transmits  $K$  pilot symbols. Bob estimates the channel gain for each transmission and collects the estimates into vector  $\hat{\mathbf{m}} = [\hat{m}_1, \dots, \hat{m}_N]$ , which is considered to be the *response* of our CR-PLA protocol.
- 4) *Verification* Bob has to decide whether the estimated vector  $\hat{\mathbf{m}}$  matches the expected gain vector  $\mathbf{m}$ , thus deciding whether the received signals were transmitted by Alice or not. This is a binary decision problem. In formulas, let  $\mathcal{H}_0$  and  $\mathcal{H}_1$  be the legitimate (null) and the under-attack hypothesis, respectively. Let  $\mathcal{H}$  the current state ( $\mathcal{H} = \mathcal{H}_0$  when Alice transmits and  $\mathcal{H} = \mathcal{H}_1$  when Trudy transmits). Given a test function  $\mathcal{E}(\mathbf{m}, \hat{\mathbf{m}})$ , the correspondent binary decision  $\hat{\mathcal{H}}$  on measurement  $\hat{\mathbf{m}}$  is

$$\hat{\mathcal{H}} = \begin{cases} \mathcal{H}_0 & \text{if } \mathcal{E}(\mathbf{m}, \hat{\mathbf{m}}) \geq \varphi, \\ \mathcal{H}_1 & \text{if } \mathcal{E}(\mathbf{m}, \hat{\mathbf{m}}) < \varphi, \end{cases} \quad (14)$$

where  $\varphi$  is a user-defined threshold. The choice of the test function is discussed in Sec. III-B.

Concerning point 2), several approaches can be performed to securely communicate the position vector  $\mathbf{x}_A$  to Alice. As a first solution, we may assume that the initial position of Alice is secret, e.g., by having Alice randomly choose that and then secretly communicate it to Bob. Next, Bob only needs to communicate the shifts from the current to the next positions  $\mathbf{x}_{n+1}$ , i.e.,  $\delta_n = \mathbf{x}_{n+1} - \mathbf{x}_n$ ,  $n = 1, \dots, N-1$ . This transmission can be public as the shift alone does not leak information on the final position. Thus, the shift vector  $\delta$  constitutes the challenge of the CR protocol to be posed to the device to be authenticated. Still, an alternative solution

could be to share  $\mathbf{x}_A$  by using a higher-level protocol for confidentiality.

Still about Step 2), we assume that for each average gain  $m \in \mathcal{M}$  there is a single corresponding position in  $\mathcal{X}$ , since the shadowing model yields a vanishing probability of having the same gain in more map positions.

#### A. Attack Model

We consider a scenario where Trudy fools Bob by picking a sequence of  $N$  positions  $\mathbf{y}_T = [y_1, \dots, y_N]$ , where  $y_n \in \mathcal{Y}$ .

Analogously to (13), we define the channel gain set for the Trudy positions' as

$$\mathcal{M}_T = \{m_T(j), j = 1, \dots, M_T\}. \quad (15)$$

Since  $M_T \geq M_A$ , we have  $\mathcal{M} \subseteq \mathcal{M}_T$ , thus Trudy chooses from a wider set of gains than Alice. We consider the worst case wherein the positions chosen by Trudy can be anywhere, also very close to Alice.

The Trudy attack is successful when it passes test (14). Hence, Trudy attack consists in i) choosing a PMD  $p_T(\mathbf{m}_T)$  of a vector  $\mathbf{m}_T = \{m_{T,1}, \dots, m_{T,N}\}$ , ii) using it to sample a vector  $\mathbf{m}_T$ , and iii) mapping it back to a sequence of positions  $\mathbf{y}_T$ .

#### B. Verification Test

We focus on the verification problem of step 4) and we resort to decision theory to optimize the test function. In the design of the test at Bob, we assume that we do not know the attack statistics, which depends on Trudy's PMD  $p_T(\mathbf{m}_T)$ . Indeed, designing a test for specific statistics is in general sub-optimal since Trudy may then deviate from it, and choose another one that may be more effective to pass test (14). Before delving into the definition of the test function  $\mathcal{E}(\mathbf{m}, \hat{\mathbf{m}})$ , let us introduce the following Lemmas.

*Lemma 1*: When Alice transmits a large number of pilot symbols ( $K \rightarrow \infty$ ), the estimated channel gain  $\hat{m}$  with Alice in position  $\mathbf{x}(i)$  has statistics

$$\hat{m} \sim \mathcal{N}\left(m(i), \frac{m(i)^2}{K}\right), \quad \text{with } m(i) \triangleq \tilde{g}_{\mathbf{x}(i)}^2 + \sigma_w^2. \quad (16)$$

*Proof*: Proof in Appendix A. ■

*Lemma 2:* Under the legitimate hypothesis  $\mathcal{H}_0$ , estimations  $\hat{m}_n$  and  $\hat{m}_{n'}$  taken at different times  $n$  and  $n'$  are statistically independent.

*Proof:* Proof in Appendix B. ■

Now, to implement (14), we resort to the log-likelihood test (LLT) test. In particular, let us define the log-likelihood for  $\mathcal{H} = \mathcal{H}_0$  given  $\mathbf{m}$  as

$$\mathcal{E}'(\hat{\mathbf{m}}, \mathbf{m}) = \log \mathbb{P}(\hat{\mathbf{m}}|\mathcal{H} = \mathcal{H}_0, \mathbf{m}) = \log p_{\mathcal{H}_0}(\hat{\mathbf{m}}|\mathbf{m}), \quad (17)$$

where  $\mathbb{P}(\cdot)$  denotes the probability operator and  $p_{\mathcal{H}_0}(\hat{\mathbf{m}}|\mathbf{m})$  is the PMD of  $\hat{\mathbf{m}}$  given the challenge  $\mathbf{m}$  when Alice is transmitting. When  $\mathcal{H} = \mathcal{H}_0$ , the entries of  $\hat{\mathbf{m}}$  are fully determined by the gains  $\mathbf{m}$  of step 2). Still, following Lemma 2, estimations relative to different transmitting positions are independent. When Alice is transmitting ( $\mathcal{H} = \mathcal{H}_0$ ), from (16) we have that  $\hat{m}_n = m_n + \tilde{w}_n$  where  $\tilde{w}_n = \mathcal{N}(0, m_n^2/K)$  and (17) becomes

$$\begin{aligned} \mathcal{E}'(\hat{\mathbf{m}}, \mathbf{m}) &= \log p_{\mathcal{H}_0}(\hat{\mathbf{m}}|\mathbf{m}) \\ &= \log \prod_{n=1}^N \frac{K}{\sqrt{2\pi m_n}} \exp\left(-\frac{K(\hat{m}_n - m_n)^2}{2m_n^2}\right) \\ &\simeq \sum_{n=1}^N \frac{K(\hat{m}_n - m_n)^2}{m_n^2} = \mathcal{E}(\hat{\mathbf{m}}, \mathbf{m}), \end{aligned} \quad (18)$$

where in the last approximation we neglected scalar factors that do not alter test (14).

We remark that, differently from the likelihood ratio test, the LLT has no optimality guarantee. Still, the test is effective and is commonly used in many security applications, e.g., [23]–[25]. Eventually, it is also possible to implement such a test without knowing the statistical description of  $\hat{\mathbf{m}}$  under  $\mathcal{H}_1$  (see [22] and [26]).

#### IV. CR-PLA OPTIMIZATION PROBLEM

The CR-PLA mechanism introduced in the previous section has several tunable parameters, in particular the test threshold  $\varphi$ , and PMDs  $p_A(\mathbf{m})$  and  $p_T(\mathbf{m}_T)$  of Bob and Trudy, respectively. All these parameters have an impact on the security and energy consumed by Alice.

In terms of security, the authentication mechanism can be characterized by the FA and MD probabilities. FA events occur when Alice's messages are considered fake and the corresponding probability is

$$P_{\text{fa}} = \mathbb{P}[\hat{\mathcal{H}} = \mathcal{H}_1 | \mathcal{H} = \mathcal{H}_0]. \quad (19)$$

A MD event occurs when Trudy messages are considered authentic and the corresponding MD probability is

$$P_{\text{md}} = \mathbb{P}[\hat{\mathcal{H}} = \mathcal{H}_0 | \mathcal{H} = \mathcal{H}_1]. \quad (20)$$

In terms of energy consumption by Alice, considering model (3), the performance can be assessed through the average traveled distance over the  $N$  rounds, i.e.,

$$\bar{D} = \mathbb{E} \left[ \sum_{n=1}^{N-1} d_{i_n, i_{n+1}} \right], \quad (21)$$

where  $i_n$  refers to the position  $\mathbf{x}(i_n)$ , i.e., the position of Alice at round  $n$  and the expectation depends on the PMD  $p_A(\mathbf{m})$ .

*Threshold Setting:* As typically done for hypothesis testing problems, we set a target FA probability and the threshold  $\varphi$  is chosen to meet this requirement. As each term of the summation in (18) is the square of an independent standard Gaussian variable,  $\mathcal{E}(\hat{\mathbf{m}}, \mathbf{m})$  is chi-squared distributed with  $N$  degrees of freedom. The FA probability is then

$$P_{\text{fa}} = \mathbb{P} \left( \sum_{n=1}^N \frac{K(\hat{m}_n - m_n)^2}{m_n^2} \geq \varphi \mid \mathbf{m} \right) = 1 - \chi_N^2(\varphi), \quad (22)$$

where  $\chi_N^2(\cdot)$  is the cumulative distribution function (CDF) of a chi-squared variable with order  $N$ . Thus, for a given desired  $P_{\text{fa}}$  we can then compute the threshold  $\varphi$  of the authentication test (14) as

$$\varphi = [\chi_N^2]^{-1}(1 - P_{\text{fa}}), \quad (23)$$

where  $[\chi_N^2]^{-1}(\cdot)$  is the inverse CDF of the chi-squared distribution with order  $N$ .

For the optimization of the PMDs, we consider both the MD probability and the average traveled distance as target. However, we assume that the security performance (in terms of MD probability) is more important than the energy performance (in terms of  $\bar{D}$ ).

For the security performance, Bob and Trudy have conflicting targets. Trudy aims at maximizing the MD probability to obtain more effective attacks, i.e.,

$$p_T^*(\mathbf{m}_T) = \arg \max_{p_T(\mathbf{m}_T)} P_{\text{md}}. \quad (24)$$

Bob instead aims at choosing the PMD  $p_A(\mathbf{m})$  to minimize the MD probability. Then, for the energy performance, among all the PMDs yielding the same MD probability Bob chooses that minimizing the average traveled distance. Thus, defining the set of PMDs minimizing the MD probability as

$$\mathcal{P}_{\text{min}} = \left\{ \hat{p}_A(\mathbf{m}) = \arg \min_{p_A(\mathbf{m})} P_{\text{md}} \right\} \quad (25)$$

we look for the PMD minimizing the average distance in this set, i.e.,

$$p_A^*(\mathbf{m}) = \arg \min_{p_A(\mathbf{m}) \in \mathcal{P}_{\text{min}}} \bar{D}. \quad (26)$$

We observe that the optimization problems (24), (25) and (26) are intertwined since the MD probability depends on both PMDs  $p_A(\mathbf{m})$  and  $p_T(\mathbf{m}_T)$ . Now, we observe that the (average) gain estimated by Bob at round  $n$  when Trudy is transmitting is

$$\hat{m}_n = z_n = m_{T,n} + \tilde{w}_{T,n}, \quad (27)$$

where  $m_{T,n} \in \mathcal{M}_T$  is the expected channel gain at round  $n$  and  $\tilde{w}_{T,n} \sim \mathcal{N}(0, m_{T,n}^2/K)$  is the estimation error (as for Alice). Thus, from the test function (18) and (27), the average MD probability can be written as

$$\begin{aligned} P_{\text{md}} &= \mathbb{E}_{\mathbf{m}, \mathbf{m}_T} \left[ \mathbb{P} \left( \sum_{n=1}^N \frac{K(z_n - m_n)^2}{m_n^2} \leq \varphi \mid \mathbf{m}, \mathbf{m}_T \right) \right] \\ &= \sum_{\mathbf{m}} \sum_{\mathbf{m}_T} \mathbb{P} \left( \sum_{n=1}^N \frac{K(z_n - m_n)^2}{m_n^2} \leq \varphi \mid \mathbf{m}, \mathbf{m}_T \right) \times \\ &\quad p_A(\mathbf{m}) p_T(\mathbf{m}_T), \end{aligned} \quad (28)$$

which depends on both PMDs.

### A. Single and Multiple Rounds

We now show that in the considered scenario both Bob and Trudy security-optimal PMD (problems (24) and (25)) yield independent gain realization at each round, i.e.,

$$\hat{p}_A(\mathbf{m}) = \prod_{n=1}^N \hat{p}_{A,n}(m_n), \quad (29)$$

$$p_T^*(\mathbf{m}_T) = \prod_{n=1}^N p_{T,n}^*(m_{T,n}). \quad (30)$$

In other words, both Bob and Trudy can extract independent gains across rounds without sacrificing security.

We start noting that Bob is agnostic of Trudy's attack PMD, i.e., he does not know  $p_T(\mathbf{m}_T)$ . Moreover, also following Lemma 2, for a given  $\mathbf{m}$ , the gain estimations in  $\hat{\mathbf{m}}$  are independent across rounds. Hence, for Bob neither Trudy nor the environment (through the noise and fading) show any dependency among rounds. Thus, his choice of the position will also be independent at each round and the PMDs constituting the set  $\mathcal{P}_{\min}$  in (25) can be written as (29).

Now, we introduce the following theorem on Trudy's optimal strategy.

*Theorem 1:* For the considered scenario, given Bob's defense PMD  $\hat{p}_A(\mathbf{m})$  as in (29), Trudy's optimal attack PMD can be factorized as in (30). In other words, Trudy's best attack is to extract independent gains at each round.

*Proof:* Proof in Appendix C. ■

From (29) and Theorem 1, both Bob and Trudy choose gains independently at each round. This implies that the joint optimization of the PMDs can be done at each round. Note however that the PMDs can be different at each round.

Thus, in the following, we focus on the case  $N = 1$ , i.e., single round, whose results are applicable also for  $N > 1$ . In this analysis, we drop the time index  $n$ , and so the single-round attack and defense PMDs become  $p_T(m_T)$  and  $p_A(m)$ .

## V. GAME MODELING AND OPTIMIZATION SOLUTION

To address the complexity of the optimization problem defined by (24)-(26), we first frame the security scenario as a game between Trudy and Bob. In the game, the target gains  $m$  and  $m_T$  represent the *actions*. Trudy aims at maximizing the MD probability, while Bob aims at minimizing it. The *mixed strategies* of the game are described by the PMDs  $p_A(m)$  and  $p_T(m_T)$ . We then characterize the strategies that constitute a NE of the game, that solve problems (24) and (25) jointly. Among those strategies, we then look for solutions to minimize the average distance traveled by Alice to solve (26).

To describe the CR-PLA mechanism as a game, let us first introduce the probability vector  $\mathbf{a}$  with length  $M_A$  and entries

$$a_i = p_A(m(i)), \quad i = 1, \dots, M_A, \quad (31)$$

and probability vector  $\mathbf{e}$  with length  $M_T$  and entries

$$e_j = p_T(m_T(j)), \quad j = 1, \dots, M_T. \quad (32)$$

The game can then be defined as follows:

- Players: Bob against Trudy.
- Sets of actions: set  $\mathcal{M}$  and  $\mathcal{M}_T$  of the gains (and so positions) Bob and Trudy can take.
- Payoff: for Trudy, the payoff obtained when Bob and Trudy play their actions (choose their positions) is the resulting MD probability  $P_{\text{md}}$ ; correspondingly for Bob the payoff is  $-P_{\text{md}}$ . The payoff matrix for Trudy is  $\mathbf{P} \in [0, 1]^{M_A \times M_T}$ , with entry (from (18) and (28))  $i = 1, \dots, M_A$ , and  $j = 1, \dots, M_T$

$$P_{i,j} = \mathbb{P} \left[ \mathcal{N} \left( \frac{(m_T(j) - m(i))\sqrt{K}}{m_T(j)}, 1 \right)^2 \leq \varphi \frac{m(i)^2}{m_T(j)^2} \right] \\ = \chi_{\text{NC}}^2 \left( \varphi \frac{m(i)^2}{m_T(j)^2}; \lambda = \frac{(m_T(j) - m(i))^2 K}{m_T(j)^2} \right), \quad (33)$$

where  $\chi_{\text{NC}}^2(\cdot; \lambda)$  is the non-central chi-squared CDF with parameter  $\lambda$ . Bob's payoff matrix is instead  $-\mathbf{P}$ .

- Strategies: the PMDs with which actions are taken by two players are  $\mathbf{a}$  and  $\mathbf{e}$ , for Bob and Trudy, respectively.
- Utility function: the utility function for Trudy is defined as

$$u_T(\mathbf{a}, \mathbf{e}) = \sum_{i=1}^{M_A} \sum_{j=1}^{M_T} P_{i,j} a_i e_j, \quad (34)$$

i.e., her expected payoff resulting from the strategies of both players. The utility of Bob instead is  $u_A(\mathbf{a}, \mathbf{e}) = -u_T(\mathbf{a}, \mathbf{e})$ . Note that the utility function of Trudy (34) is equivalent to (28) (with  $N = 1$ ).

In game theory, a strategy is pure when the probability distribution is degenerate, e.g., for Bob  $a_i = 1$  for some  $i$  and 0 otherwise; in all the other cases (including our game) the strategy is *mixed*. Note that Bob and Trudy choose a strategy, not an action: these two concepts are the same only for a pure strategy.

The game can be classified as a static *zero-sum* game of complete information. It is static because there is no time dependency and single-shot moves fully determine the outcome of the game. It is a zero-sum game because the two players have opposite objectives, i.e.,  $u_A(\mathbf{a}, \mathbf{e}) = -u_T(\mathbf{a}, \mathbf{e})$ . It has complete information since the sets of actions and the payoffs are common knowledge.

### A. Nash Equilibrium Characterization

We recall that strategies  $(\mathbf{a}^*, \mathbf{e}^*)$  are a NE (i.e., optimal from a game theory perspective) if there is no unilateral deviation of the players leading to a better utility. In formulae, if  $(\mathbf{a}^*, \mathbf{e}^*)$  is a NE, then

$$u_A(\mathbf{a}^*, \mathbf{e}^*) \geq u_A(\mathbf{a}, \mathbf{e}^*) \quad \forall \mathbf{a}, \quad (35)$$

and

$$u_T(\mathbf{a}^*, \mathbf{e}^*) \geq u_T(\mathbf{a}^*, \mathbf{e}) \quad \forall \mathbf{e}. \quad (36)$$

We now characterize the set of NE strategies for the considered game. To this end, let us define the maximin

problem, where Bob first optimizes his strategy and then Trudy optimizes her strategy as

$$u_{T,\max}^* = \max_e \min_a u_T(\mathbf{a}, \mathbf{e}). \quad (37)$$

Similarly, let us define the minimax problem, where Trudy first optimizes his strategy and then Bob optimizes his strategy as

$$u_{T,\min}^* = \min_a \max_e u_T(\mathbf{a}, \mathbf{e}). \quad (38)$$

Let us also define Trudy's strategies  $\mathbf{e}_{\max}$  and  $\mathbf{e}_{\min}$  that lead to the  $u_{T,\max}^*$  (37) and  $u_{T,\min}^*$  (38), respectively.

Since the game is zero-sum, the following results hold:

- 1) As the set of actions is finite, at least one NE exists in mixed strategies [27, Sec. 6.4].
- 2) From the minimax theorem [28], we have

$$\mathbf{e}^* = \mathbf{e}_{\max} = \mathbf{e}_{\min}, \quad u^* = u_{T,\min}^* = u_{T,\max}^*. \quad (39)$$

- 3) *Lemma 3:* All NEs yield the same utility.

*Proof:* Proof in Appendix D. ■

### B. Game-Based Optimization Problem

From (39), we can compute the utility of any NE by solving the maximin problem (37) via linear programming as shown in [29, Sec. 3.10]. In particular, by letting  $\mathbf{P}_i^T$  to be the  $i$ -th row of  $\mathbf{P}$ , the NE utility is the solution of the following optimization problem

$$\begin{aligned} u^* = \max_u \quad & u \\ \text{s.t.} \quad & u \leq \mathbf{P}_i^T \mathbf{e}, \quad \forall i \in 1, \dots, M_A, \\ & \sum_{j=1}^{M_T} e_j = 1, \quad e_j \geq 0, \forall j. \end{aligned} \quad (40)$$

Note that the utility of the game  $u^*$  coincides with the average MD probability of (28) and  $\mathbf{e}^*$  (i.e., the solution of (40) achieving  $u^*$ ) is an optimal solution for Trudy.

As Bob's utility is the opposite of Trudy, we now have a characterization of the set  $\mathcal{P}_{\min}$  in (25), as the set of strategies solving (40) with  $-\mathbf{P}^T$  in place of  $\mathbf{P}$  (see [29, Sec. 3.10]), thus we have

$$\mathcal{P}_{\min} = \{\mathbf{a} : -\mathbf{P}^T \mathbf{a} \geq u^* \mathbf{1}\}, \quad (41)$$

where  $\mathbf{1}$  is the vector with all entries equal to 1. We will use this result to find the minimum-distance best response for Bob, in the next subsections.

### C. Multi-Round Multiple-NE Solution

We now consider again the optimization problem (24)-(26) with multiple rounds. We denote as  $\mathbf{a}^*(i, n)$  the optimal distribution to use when Alice is located in position  $\mathbf{x}(i)$  at round  $n$ . Specifically, each element  $a_{i'}^*(i, n)$  is the optimal probability of moving to position  $\mathbf{x}(i')$  at round  $n+1$  given Alice is located in position  $\mathbf{x}(i)$  at round  $n$ . We denote as  $\mathbf{A}^*(n)$  the  $M_A \times M_A$  matrix whose column  $i$  is the vector  $\mathbf{a}^*(i, n)$ , i.e.,  $\mathbf{A}^*(n)_{:,i} = \mathbf{a}^*(i, n)$ , that collects all the optimal strategies at round  $n$  for each Alice position. Next, we collect in  $\mathbf{A}^* = [\mathbf{A}^*(1), \dots, \mathbf{A}^*(N)]$  that contains the optimal strategies for each position, at each round. By defining

the probability of extracting a sequence of position indexes  $\mathcal{I} = \{i_1, \dots, i_N\}$  as  $p_{\mathcal{I}}(\mathcal{I}, \mathbf{A}) = \prod_{n=1}^{N-1} a_{i_{n+1}}(i_n, n)$ , the optimization problem (26) can be rewritten as

$$\begin{aligned} \mathbf{A}^* = \arg \min_{\mathbf{A}} \quad & \sum_{\mathcal{I}=\{i_1, \dots, i_N\}} \left[ \sum_{n=1}^{N-1} d_{i_n, i_{n+1}} \right] p_{\mathcal{I}}(\mathcal{I}, \mathbf{A}) \\ \text{s.t.} \quad & \forall i \in 1, \dots, M_A, \forall n : \\ & u^* \mathbf{1} \leq -\mathbf{P}^T \mathbf{a}(i, n) \\ & \sum_{i'=1}^{M_A} a_{i'}(i, n) = 1, \quad \mathbf{a}(i, n) \geq \mathbf{0}. \end{aligned} \quad (42)$$

We denote the solution of problem (42) as multi-round multiple (MRM)-NE solution.

We note that problem (42) is non-convex and has a large number of variables ( $M_A^2 N$ ); moreover, the number of operations to evaluate the objective function is  $2NM_A^N$ . Thus, in the following, we present a relaxed version of (42) that can be solved with lower complexity.

### D. Single-Hop Multiple-NE Solution

As we will see in Section VI, even with a small number of rounds ( $N = 2, 3$ ) we achieve a low MD probability. This suggests that, instead of optimizing over multiple rounds, we could neglect the effect of choosing a position at round  $n$  on the distance traveled on subsequent rounds. In other words, we could neglect time in the optimization, and apply the same strategy at each round (see [11]). Thus we simplify (42) by finding a NE that depends solely on Alice's current position, thus we have  $\mathbf{a}^*(i, n) = \mathbf{a}^*(i)$ . For each position  $\mathbf{x}(i)$ , the corresponding NE that minimizes the average distance traveled when the drone is in that position is

$$\begin{aligned} \mathbf{a}^*(i) = \arg \min_{\mathbf{a}(i)} \quad & \sum_{i'=1}^{M_A} d_{i,i'} a_{i'}(i) \\ \text{s.t.} \quad & u^* \mathbf{1} \leq -\mathbf{P}^T \mathbf{a}(i) \\ & \sum_{i'=1}^{M_A} a_{i'}(i) = 1, \quad \mathbf{a}(i) \geq \mathbf{0}. \end{aligned} \quad (43)$$

We denote this problem as single-hop multiple (SHM)-NE solution.

Note that to find the optimal strategy  $\mathbf{A}^*(n) = \mathbf{A}^*$  we need to solve (43)  $M_A$  times (one for each starting position  $\mathbf{x}(i)$ ), but each solution is optimal and much easier to compute than (42), since (43) is a linear program.

### E. Single NE Solution

In this last approach, we find a single NE  $\mathbf{a}^*$  that minimizes the average traveled distance, without taking into account the current and next positions, thus in a greedy fashion. Consequently we have  $\mathbf{a}^*(i, n) = \mathbf{a}^*$ . Let us define the distance matrix  $\mathbf{D} \in \mathbb{R}^{M_A \times M_A}$ , whose entries (from (4)) are

$$D_{i,i'} = d_{i,i'} \quad \text{for } i, i' = 1, \dots, M_A. \quad (44)$$

TABLE I  
SIMULATION PARAMETERS

Symbol	Description	Default value
$K$	Number of pilots symbols	50
$N$	Number of rounds	1
$\sigma_{(s)\text{dB}}$	Shadowing STD	10 dB
$h$	Altitude	50 m
$M_A$	Number of Alice positions	$15 \times 15$
$M_T$	Number of Trudy positions	$15 \times 15$
$f_c$	Carrier frequency	2.4 GHz

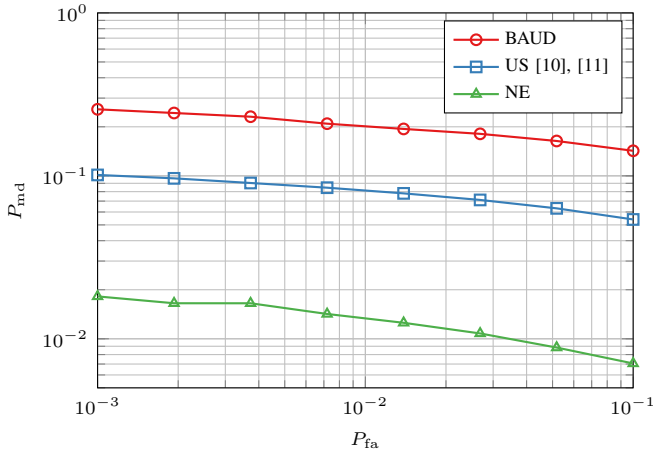


Fig. 2. DET curve of the proposed protocol with different strategies and  $N = 2$  rounds.

Given a mixed strategy  $\mathbf{a}$  for Bob, we compute the average traveled distance as

$$\begin{aligned} \bar{D}(\mathbf{D}, \mathbf{a}) &= \sum_{i=1}^{M_A} \sum_{i'=1}^{M_A} d_{i,i'} a_i a_{i'} \\ &= \mathbf{a}^T \mathbf{D} \mathbf{a}, \end{aligned} \quad (45)$$

The optimization problem thus becomes

$$\begin{aligned} \mathbf{a}^* &= \arg \min_{\mathbf{a}} \mathbf{a}^T \mathbf{D} \mathbf{a} \\ \text{s.t. } & \mathbf{u}^* \mathbf{1} \leq -\mathbf{P}^T \mathbf{a} \\ & \sum_{i'=1}^{M_A} a_{i'} = 1, \mathbf{a} \geq \mathbf{0}, \end{aligned} \quad (46)$$

We denote problem (46) as single NE (S-NE) solution.

Since  $\mathbf{D}$  is not positive semidefinite, (46) is not convex. Consequently, we solve it with a sequential least squares programming (SLSQP) approach [30].

## VI. NUMERICAL RESULTS

In this section, we report simulation results of the proposed CR-PLA with optimized strategies, and compare them with existing techniques. We consider a scenario wherein both Trudy and Alice move on a square grid of dimension  $420 \text{ m} \times 420 \text{ m}$  at a fixed height  $h$ . The values of shadowing STDs  $\sigma_{(s)\text{dB}}$  are taken from [31], where a ray-tracing simulation is used to

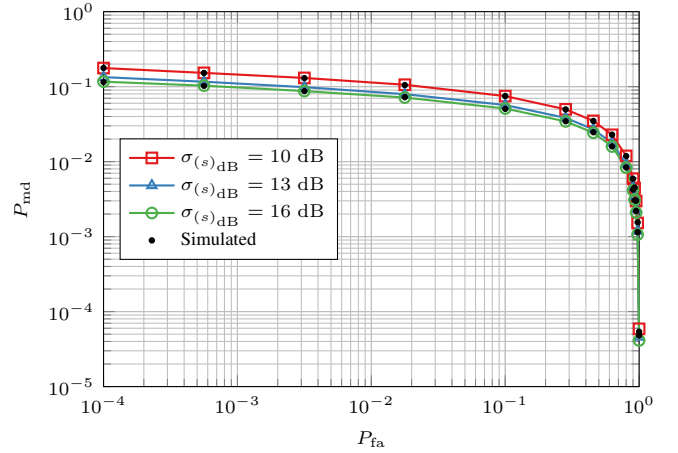


Fig. 3. DET curves for  $\sigma_{(s)\text{dB}} = 10, 13,$  and  $16$  dB.

model a channel at 2.4 GHz in different environments. Values  $\sigma_{(s)\text{dB}} \simeq 10, 13,$  and  $16$  dB refers to urban and suburban not line-of-sight (NLOS) scenarios, respectively. Table I summarizes the main simulation parameters; if not otherwise stated, the parameters used in the simulations are reported in the column *Default value*.

### A. Comparison With Other Approaches

We first compare the security performance of our scheme with other solutions present in the literature. In particular, we consider the uniform strategy (US) proposed in [10] and [11], where Bob and Trudy uniformly pick a gain over the set of possible values of the map. We also consider the case in which Bob still picks the gain uniformly at random, while Trudy uses the strategy that maximizes the MD probability: this is the best attack against the uniform defense strategy proposed in [10], [11] and we denote it as the best attack against the uniform defense (BAUD) strategy.

Note that the various solutions discussed in Section V achieve all the same security performance since we always consider NEs of the game, and all NEs yield the same MD probability.

Fig. 2 reports the detection error trade-off (DET) curves, i.e., MD probability as a function of the FA probability, considering the proposed game theoretic approach (denoted with NE in the plot) against the US and BAUD strategies. The number of rounds is  $N = 2$ , while the other parameters are reported in Table I. We confirm that the NE provides the lowest MD probability, as the uniform strategy is not the best for Bob. Moreover, we see that the uniform strategy for Bob is particularly vulnerable to the best attack by Trudy. We also observe that we are able to reduce the MD probability by one order or magnitude with just two rounds.

### B. Impact of CR-PLA Parameters

We now investigate the effects of several parameters of the proposed technique on its performance.



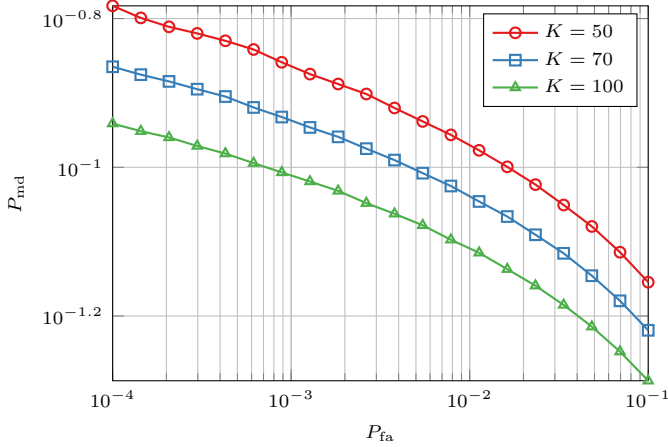


Fig. 4. DET curves for different number of pilot symbols,  $K$ .

*Shadowing variance  $\sigma_{(s)\text{dB}}$* : first, Fig. 3 compares the security performance in environments characterized by different shadowing variances. The figure shows the DET curves, for  $N = 1$ ,  $\sigma_{(s)\text{dB}} = 10, 13$ , and  $16$  dB. Lines are obtained with the close-form formulas of the probability, while black markers show the results obtained with simulations. We note a perfect agreement between the analytical and numerical results. When comparing the different variances of the shadowing, we note that the MD probability decreases with  $\sigma_{(s)\text{dB}}$  (for a fixed FA probability). This is because a high  $\sigma_{(s)\text{dB}}$  value increases the map diversity, i.e., positions at the same distance from the receiver have different gains, thus it is harder for Trudy to guess a position leading to the same gain as Alice to fool Bob.

In the next figures, we will keep the shadowing variance fixed to  $\sigma_{(s)\text{dB}} = 10$  dB.

*Number of Pilot Symbols  $K$* : We now consider the impact of the number of pilot symbols used for channel estimation in the authentication phase of CR-PLA. Fig. 4 shows the DET curves of the proposed solution for  $N = 1$  round and  $K = 50, 70$ , and  $100$  pilot symbols. We see that a higher  $K$  yields better channel estimates and thus lower MD probabilities. However, the benefits are limited, indicating that it may be possible to achieve a good security performance even with low  $K$  values, thus potentially saving drone energy and time.

*Number of Rounds  $N$* : We now consider the impact of the number of rounds  $N$  on the security performance. Fig. 5 shows the MD probability as a function of rounds  $N$  for FA probabilities  $10^{-2}, 10^{-3}$ , and  $10^{-4}$ . From the results we see that the MD decreases exponentially with the number of rounds, thus we can easily reduce the MD probability to desired values by adding a few more rounds. This however comes at the cost of an increased consumed energy, as discussed below.

### C. Impact of The Map Geometry

We now investigate the maps' effects on the proposed solution's performance.

*Drone Altitude*: First, we investigate the impact of Alice's and Trudy's altitude  $h$ . Fig. 6 shows the achieved average

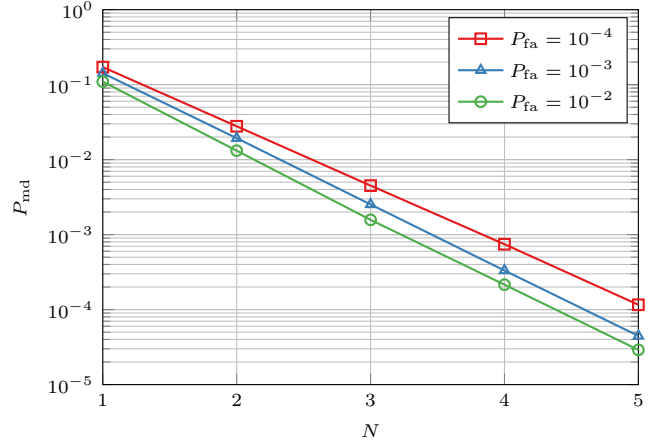


Fig. 5.  $P_{\text{md}}$  as a function of the number of rounds,  $N$ , for  $P_{\text{fa}} = 10^{-2}, 10^{-3}$ , and  $10^{-4}$ .

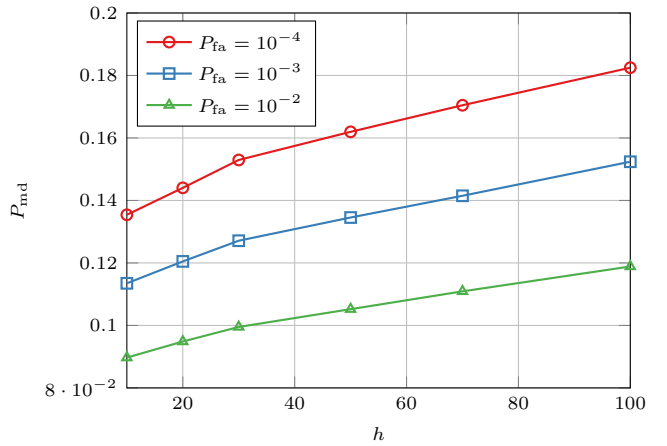


Fig. 6.  $P_{\text{md}}$  as a function of the drone altitude,  $h$ , for  $P_{\text{fa}} = 10^{-3}$ .

$P_{\text{md}}$  as a function of  $h$ , for  $P_{\text{fa}} = 10^{-2}, 10^{-3}$ , and  $10^{-4}$ , and  $N = 1$  round. We note that the MD probability slightly increases with  $h$ : indeed, increasing the altitude decreases the gain map diversity as the grid area is fixed. In fact, the path loss becomes less relevant as all the grid positions experience the same path loss as the altitude  $h$  increases. This leads to a reduced variance of the gains over the map, and thus more similar challenges/responses, which in turn makes it easier for Trudy to guess the correct response.

*Number of Positions of the Map*: Then, we consider the impact of the number of positions on map, here  $\mathcal{X} = \mathcal{Y}$ . Fig. 7 shows the MD probability as a function of the number of grid positions for  $P_{\text{fa}} = 10^{-2}, 10^{-3}$ , and  $10^{-4}$ , and  $N = 1$  round. We note that by increasing the overall number of positions (thus the number of possible challenges) the MD probability decreases. Still, after a rapid decrease, the MD reaches a plateau. Indeed, as the number of positions increases we obtain a gain map with very similar gains that do not provide significant diversity to the authentication process. Still, the results highlight the trade-off between the duration of Step 1) of the protocol (see Section III) and the achievable performance, while showing that i) it is not necessary to

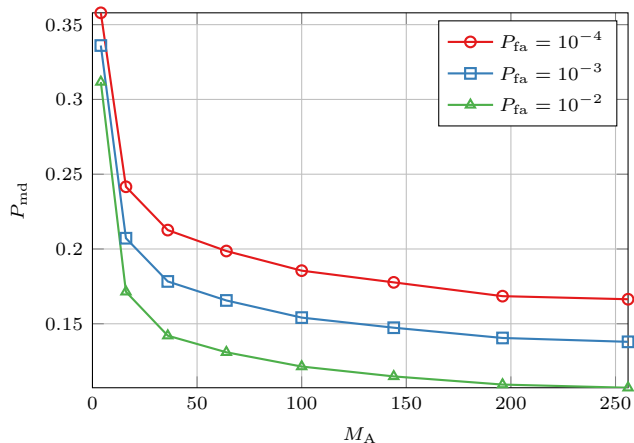


Fig. 7.  $P_{\text{md}}$  as function of the number of grid positions, for  $P_{\text{fa}} = 10^{-2}$ ,  $10^{-3}$ , and  $10^{-4}$ .

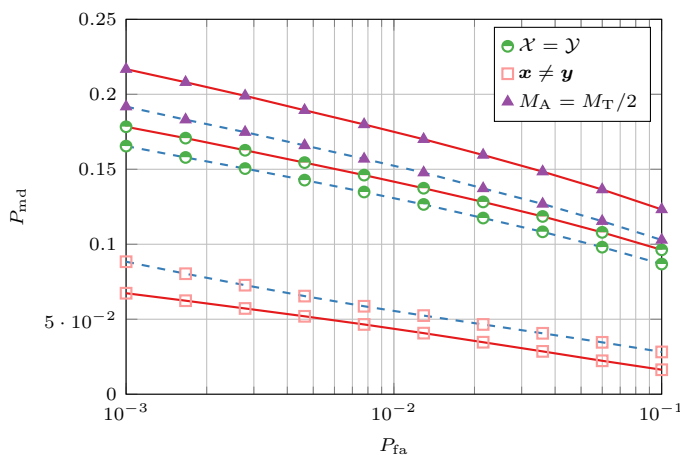


Fig. 8. DET curves with  $M_T = 36$  (solid) and  $M_T = 64$  (dashed) and various type of Alice-Trudy maps.

sample too finely the space to achieve good performance and ii) a too precise sampling does not necessarily bring benefits for the legitimate party.

*Alice-Trudy Map Difference:* We study the impact that different sets of positions available to Trudy and Alice have on the DET curves. In particular, we consider a scenario wherein the positions in  $\mathcal{X}$  are half of those in  $\mathcal{Y}$ ,  $M_A = M_T/2$ , and Alice positions are selected uniformly at random from Trudy's map. We denote this scenario as  $M_A = M_T/2$  and compare it with a scenario in which Alice and Trudy have the same map (denoted as  $\mathcal{X} = \mathcal{Y}$ ). Lastly, we consider the case in which the maps of Alice and Trudy are the same, but Trudy is not allowed to select the same position as Alice (as this may lead to a clash), and denote this scenario as  $x \neq y$ . Fig. 8 shows the DET for the three considered cases, comparing the results for  $M_T = 36$  and  $64$ , for  $N = 1$ . We can see that when Alice's map has half of the positions of Trudy, the  $P_{\text{md}}$  increases, as expected. Still, there are no big differences even though the number of grid positions is halved for Alice: this suggests that as long as there is enough variability in the gains available, Bob is still able to achieve good security performance. This fact is also confirmed by the scenario where Trudy is deprived

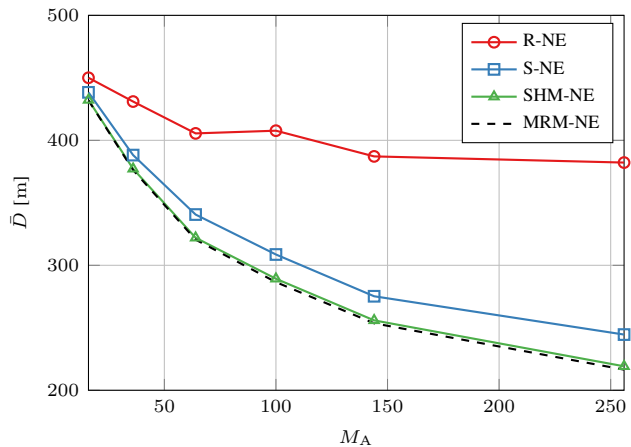


Fig. 9. Average distance traveled by Alice with respect to the number of grid positions  $M_A$ , with  $N = 2$  rounds, for  $P_{\text{fa}} = 10^{-3}$ .

of "good" positions (i.e., excluding the case where she's in the same Alice's location) where we see that it improves the performance. These effects are more visible when there are fewer grid positions. Indeed, the denser the grid the less likely it is that the deleted positions are relevant.

#### D. Average Traveled Distance

We now discuss the effectiveness of the distance minimization algorithms. We consider the S-NE, the optimal MRM-NE, and the SHM-NE solutions. For comparison purposes we also show the average distance for a NE without distance optimization, a random NE is selected at each round (R-NE).

Fig. 9 shows the average distance  $\bar{D}$  traveled by Alice over  $N = 2$  rounds, as a function of the number of positions of the map  $M_A$ , positioned on a grid always occupying the same area. As we can see the distance-optimized solutions outperform the baseline R-NE, and by increasing the number of grid positions the distance traveled reduces. This is because by increasing the positions the more degrees of freedom the optimization algorithms have, thus can find better NEs from the distance perspective. We also notice that the SHM-NE solution outperforms the S-NE solution and achieves close-to-bound performance (represented by the optimal MRM-NE solution) but with much lower computations, confirming our suppositions.

## VII. CONCLUSIONS

In this paper, we have proposed novel strategies for CR-PLA with drones: we have optimized the PMD used to select the challenge by Bob, and correspondingly the PMD of the random attack performed by Trudy. We formulated the problem as a zero-sum game with payoff the MD probability, then characterizing the NEs of the game. To further decrease the MD probability the protocol can be repeated for multiple rounds/movements.

Among solutions providing the same MD probability, we have then selected the PMD for Bob yielding the minimum energy consumption due to the movement. Three solutions

were proposed: the optimal MRM-NE solution, the S-NE solution where the challenge is chosen drawing always the same NE, and the SHM-NE solution where we associate the best NE to each possible position on the map. SHM-NE performs close to the optimal MRM-NE strategy, but it is much more lightweight in terms of computations.

Simulation results are performed by generating a realistic shadowing map, which includes both path loss and fading, modeling a realistic urban NLOS scenario. In particular, the proposed solution achieves MD/FA probabilities of  $\sim 10^{-3}$  with only  $N = 3$  rounds.

## REFERENCES

- [1] M. Adil, M. A. Jan, Y. Liu, H. Abulkasim, A. Farouk, and H. Song, "A systematic survey: Security threats to UAV-aided IoT applications, taxonomy, current challenges and requirements with future research directions," *IEEE Trans. Intell. Transp. Syst.*, vol. 24, no. 2, pp. 1437–1455, Feb. 2023.
- [2] M. Ceccato, F. Formaggio, and S. Tomasin, "Spatial GNSS spoofing against drone swarms with multiple antennas and Wiener filter," *IEEE Trans. Signal Process.*, vol. 68, pp. 5782–5794, Oct. 2020.
- [3] G. Michieletto, F. Formaggio, A. Cenedese, and S. Tomasin, "Robust localization for secure navigation of UAV formations under GNSS spoofing attack," *IEEE Trans. Automat. Sci. and Eng.*, pp. 1–14, Sept. 2022.
- [4] E. Illi, M. Qaraqe, S. Althunibat, A. Alhasanat, M. Alsafasfeh, M. de Ree, G. Mantas, J. Rodriguez, W. Aman, and S. Al-Kuwari, "Physical layer security for authentication, confidentiality, and malicious node detection: A paradigm shift in securing IoT networks," *IEEE Commun. Surv. & Tut.*, vol. 26, no. 1, pp. 347–388, Firstquarter 2024.
- [5] T. M. Hoang, A. Vahid, H. D. Tuan, and L. Hanzo, "Physical layer authentication and security design in the machine learning era," *IEEE Commun. Surv. & Tut.*, vol. 26, no. 3, pp. 1830–1860, Thirdquarter 2024.
- [6] S. J. Maeng, Y. Yapıcı, I. Güvenç, H. Dai, and A. Bhuyan, "Power allocation for fingerprint-based PHY-layer authentication with mmWave UAV networks," in *Proc. of the Int. Conf. on Commun. (ICC)*, 2021, pp. 1–6.
- [7] A. Yazdinejad, R. M. Parizi, A. Dehghantaha, and H. Karimipour, "Federated learning for drone authentication," *Ad Hoc Netw.*, vol. 120, p. 102574, Sept. 2021.
- [8] P. C. Gupta, *Cryptography and network security*. PHI Learning, 2014.
- [9] S. Tomasin, H. Zhang, A. Chorti, and H. V. Poor, "Challenge-response physical layer authentication over partially controllable channels," *IEEE Commun. Mag.*, vol. 60, no. 12, pp. 138–144, Dec. 2022.
- [10] F. Mazzo, S. Tomasin, H. Zhang, A. Chorti, and H. V. Poor, "Physical-layer challenge-response authentication for drone networks," in *Proc. of IEEE Global Commun. Conf. (GLOBECOM)*, 2023, pp. 3282–3287.
- [11] F. Ardizzon, D. Salvaterra, M. Piana, and S. Tomasin, "Energy-based optimization of physical-layer challenge-response authentication with drones," [Accepted] *Proc. of IEEE Global Commun. Conf. (GLOBECOM)*, 2024. [Online]. Available: <https://arxiv.org/abs/2405.03608>
- [12] H. V. Abeywickrama, B. A. Jayawickrama, Y. He, and E. Dutkiewicz, "Comprehensive energy consumption model for unmanned aerial vehicles, based on empirical studies of battery performance," *IEEE Access*, vol. 6, pp. 58383–58394, Oct. 2018.
- [13] Y. Zhang, D. He, L. Li, and B. Chen, "A lightweight authentication and key agreement scheme for Internet of Drones," *Comput. Commun.*, vol. 154, pp. 455–464, Mar. 2020.
- [14] L. Xiao, T. Chen, G. Han, W. Zhuang, and L. Sun, "Channel-based authentication game in MIMO systems," in *Proc. of IEEE Global Commun. Conf. (GLOBECOM)*, 2016, pp. 1–6.
- [15] Y. Ge and Q. Zhu, "GAZETA: Game-theoretic zero-trust authentication for defense against lateral movement in 5G IoT networks," *IEEE Trans. on Inf. Forens. and Secur.*, vol. 19, pp. 540–554, Oct. 2024.
- [16] Y. Wu, T. Jing, Q. Gao, Y. Wu, and Y. Huo, "Game-theoretic physical layer authentication for spoofing detection in Internet of Things," *Digit. Commun. and Netw.*, Jan. 2023.
- [17] Y. Zhou, P. L. Yeoh, K. J. Kim, Z. Ma, Y. Li, and B. Vucetic, "Game theoretic physical layer authentication for spoofing detection in UAV communications," *IEEE Trans. on Veh. Technol.*, vol. 71, no. 6, pp. 6750–6755, Mar. 2022.
- [18] M. Gudmundson, "Correlation model for shadow fading in mobile radio systems," *Electron. Lett.*, vol. 23, no. 27, pp. 2145–2146, Nov. 1991.
- [19] N. Benvenuto, G. Cherubini, and S. Tomasin, *Algorithms for Commun. Systems and their Applications*, 2nd ed. Wiley, 2021.
- [20] D. Tse and P. Viswanath, *Fundamentals of wireless communication*. Cambridge University Press, 2005.
- [21] R. H. Clarke, "A statistical theory of mobile-radio reception," *The Bell Syst. Tech. J.*, vol. 47, no. 6, pp. 957–1000, July-Aug. 1968.
- [22] L. Senigagliales, M. Baldi, and E. Gambi, "Comparison of statistical and machine learning techniques for physical layer authentication," *IEEE Trans. Inf. Forensics Secur.*, vol. 16, pp. 1506–1521, Oct. 2021.
- [23] L. Bragagnolo, F. Ardizzon, N. Laurenti, P. Casari, R. Diamant, and S. Tomasin, "Authentication of underwater acoustic transmissions via machine learning techniques," in *Proc. of IEEE Int. Conf. on Microw., Antennas, Commun. and Electron. Syst. (COMCAS)*, 2021, pp. 255–260.
- [24] L. Chiarello, P. Baracca, K. Upadhyaya, S. R. Khosravirad, and T. Wild, "Jamming detection with subcarrier blanking for 5G and beyond in industry 4.0 scenarios," in *Proc. Annu. Int. Symp. on Pers., Indoor and Mobile Radio Commun. (PIMRC)*, 2021, pp. 758–764.
- [25] X. Peng, C. Huang, X. Zhu, Z. Chen, and X. Yuan, "GLRT-based spacetime detection algorithms via joint DoA and Doppler shift method for GNSS spoofing interference," *IEEE Internet Things J.*, pp. 1–1, June 2024.
- [26] F. Ardizzon and S. Tomasin, "Learning the likelihood test with one-class classifiers for physical layer authentication," 2024. [Online]. Available: <https://arxiv.org/abs/2210.12494>
- [27] S. Tadelis, *Game theory: an introduction*. Princeton University Press, 2013.
- [28] J. V. Neumann, "Zur Theorie der Gesellschaftsspiele," *Math. Ann.*, vol. 100, no. 1, pp. 295–320, Dec. 1928.
- [29] A. Washburn, *Two-person zero-sum games*. Springer, 2014.
- [30] P. T. Boggs and J. W. Tolle, "Sequential quadratic programming," *Acta Numer.*, vol. 4, p. 1–51, 1995.
- [31] N. Sharma, M. Magarini, L. Dossi, L. Reggiani, and R. Nebuloni, "A study of channel model parameters for aerial base stations at 2.4 GHz in different environments," in *Proc. IEEE Annu. Consumer Commun. & Netw. Conf. (CCNC)*, 2018, pp. 1–6.

## APPENDIX A PROOF OF LEMMA 1

From (12) with  $\mathbf{q} = \mathbf{x}(i)$ , let

$$\tilde{r}_k = \tilde{g}_{\mathbf{x}(i)} h_k e^{-j\phi} + w'_k. \quad (47)$$

We note that real and imaginary parts of  $\tilde{r}_k$  are zero-mean Gaussian distributed random variables with variance

$$\tilde{\sigma}_{\mathbf{x}(i)}^2 = \frac{\tilde{g}_{\mathbf{x}(i)}^2 + \sigma_w^2}{2}, \quad (48)$$

which depends on Alice's position  $\mathbf{x}(i)$ . Consequently,  $|\tilde{r}_k|^2$  is exponentially distributed with parameter

$$\lambda_{\mathbf{x}(i)} = \frac{1}{2\tilde{\sigma}_{\mathbf{x}(i)}^2}. \quad (49)$$

We assume that the samples  $r_k$  of the received signal are taken sufficiently far apart in time, i.e., with  $T_s > T_c$ , so the fading coefficients  $h_k$  are statistically independent. This implies that

$$\mathbb{E}[\tilde{r}_k \tilde{r}_{k'}^*] = 0, \forall k' \neq k, \quad (50)$$

thus samples taken at different times  $k$  and  $k'$  are independent, since  $\tilde{r}_k$  is Gaussian. Hence, we resort to the central limit theorem, thus  $\mu(\mathbf{x}(i))$ , defined in (12), converges, for  $K$  sufficiently large, in terms of CDF to a normal distribution

$$\sqrt{K} \left( \mu(\mathbf{x}(i)) - \frac{1}{\lambda_{\mathbf{x}(i)}} \right) \xrightarrow{d} \mathcal{N} \left( 0, \frac{1}{\lambda_{\mathbf{x}(i)}^2} \right). \quad (51)$$

Lastly, reordering the terms and defining  $m(i) = 1/\lambda_{\mathbf{x}(i)}$ , we obtain (16).

APPENDIX B  
PROOF OF LEMMA 2

From (12) and (47), two gains  $\hat{m}_n$  and  $\hat{m}_{n'}$  estimated by Bob at different times  $n = kT_s$  and  $n' = k'T_s$  have correlation

$$\begin{aligned} \mathbb{E}[\hat{m}_n \hat{m}_{n'}] &= \mathbb{E} \left[ \frac{1}{K} \sum_k |\tilde{r}_k|^2 \frac{1}{K} \sum_{k'} |\tilde{r}_{k'}|^2 \right] \\ &= \frac{1}{K^2} \sum_k \sum_{k'} \mathbb{E} [|\tilde{r}_k|^2 |\tilde{r}_{k'}|^2]. \end{aligned} \quad (52)$$

Next, as discussed in Appendix A, samples  $\tilde{r}_k$  and  $\tilde{r}_{k'}$  measured at sufficiently far apart instants, and therefore also their squared amplitude, are independent, hence reordering the terms

$$\begin{aligned} \mathbb{E}[\hat{m}_n \hat{m}_{n'}] &= \frac{1}{K^2} \sum_k \sum_{k'} \mathbb{E} [|\tilde{r}_k|^2 |\tilde{r}_{k'}|^2] \\ &= \frac{1}{K^2} \sum_k \sum_{k'} \mathbb{E} [|\tilde{r}_k|^2] \mathbb{E} [|\tilde{r}_{k'}|^2] = \mathbb{E}[\hat{m}_n] \mathbb{E}[\hat{m}_{n'}]. \end{aligned} \quad (53)$$

From (53), we have that  $\hat{m}_n$  and  $\hat{m}_{n'}$  are uncorrelated, thus independent as they are Gaussian.

APPENDIX C  
PROOF OF THEOREM 1

As discussed in Section IV-A, Bob draws her gains independently, thus (29) holds. Given that Bob's and Trudy's PMDs are independent from each other, the MD probability can be written as

$$P_{\text{md}} = \sum_{\mathbf{m}} \sum_{\mathbf{m}_T} \mathbb{P} \left( \sum_{n=1}^N \frac{K(\hat{m}_n(\mathbf{m}_T) - m_n)^2}{m_n^2} \leq \varphi \middle| \mathbf{m}, \mathbf{m}_T \right) \times p_A(\mathbf{m}) p_T(\mathbf{m}_T), \quad (54)$$

where (54) is (28) highlighting the fact that, in general, the measured gain when Trudy is transmitting may be a function of the previous (or next) gains, i.e.,  $z_n = z_n(\mathbf{m}_T) = \hat{m}_n(\mathbf{m}_T)$ .

Focusing on the choice of  $m_{T,k}$ ,  $k = 1, \dots, N$ , let  $\bar{\mathbf{m}}_T$  be the vector  $\mathbf{m}_T$  from which we exclude the  $k$ -th entry  $m_{T,k}$ . Next, we define

$$\phi(\bar{\mathbf{m}}_T, \mathbf{m}) = \sum_{n=1, n \neq k}^N \frac{K(\hat{m}_n(m_{T,n}) - m_n)^2}{m_n^2}, \quad (55)$$

representing the results of all the tests except the  $k$ -th test.

To prove the theorem, we focus on the latter term in (54). In particular, we split the  $k$ -th test result from the others exploiting (55), as

$$\begin{aligned} &\mathbb{P} \left( \sum_{n=1}^N \frac{K(\hat{m}_n(\mathbf{m}_T) - m_n)^2}{m_n^2} \leq \varphi \middle| \mathbf{m}, \mathbf{m}_T \right) = \\ &\mathbb{P}(\phi(\bar{\mathbf{m}}_T, \mathbf{m}) = \phi|\bar{\mathbf{m}}_T, \mathbf{m}) \times \\ &\mathbb{P} \left( \frac{K(\hat{m}_k(m_{T,k}) - m_k)^2}{m_k^2} \leq \varphi - \phi \middle| m_k, m_{T,k}, \phi \right) \end{aligned} \quad (56)$$

Now, noticed that in (54) it holds

$$p_T(\mathbf{m}_T) = \mathbb{P}(m_{T,k} | \bar{\mathbf{m}}_T) \mathbb{P}(\bar{\mathbf{m}}_T), \quad (57)$$

by reordering the terms in (54), we can define the probability

$$f(\mathbf{m}_T, \mathbf{m}) = \mathbb{P}(m_{T,k} | \bar{\mathbf{m}}_T) \times \mathbb{P} \left( \frac{K(\hat{m}_k(m_{T,k}) - m_k)^2}{m_k^2} \leq \varphi - \phi \middle| m_k, m_{T,k}, \phi \right), \quad (58)$$

which groups together all the terms that are impacted by the choice of the gain  $m_{T,k}$  at round  $k$  in (54). We note that  $m_n$  are independent and that the maximization of this probability depends on neither  $\varphi$  nor  $\phi$ . In other words, this shows that on each round Trudy aims at maximizing (58), regardless of the previous and next choices.

Finally, we can conclude that each round is an independent game that can be solved separately, i.e., the overall attacker PMD can be factorized as in (30).

APPENDIX D  
PROOF OF LEMMA 3

Let  $(\mathbf{a}_1^*, \mathbf{e}_1^*)$  and  $(\mathbf{a}_2^*, \mathbf{e}_2^*)$  be two NEs. Then, by definition of NE, we have that

$$\begin{aligned} u_A(\mathbf{a}_1^*, \mathbf{e}_1^*) &\geq u_A(\mathbf{a}_2^*, \mathbf{e}_1^*), \\ u_T(\mathbf{a}_1^*, \mathbf{e}_1^*) &\geq u_T(\mathbf{a}_1^*, \mathbf{e}_2^*). \end{aligned} \quad (59)$$

Since the game is zero-sum, we have  $u_T = -u_A$ , thus  $u_A(\mathbf{a}_2^*, \mathbf{e}_1^*) \geq u_A(\mathbf{a}_2^*, \mathbf{e}_2^*)$ . Hence

$$u_A(\mathbf{a}_1^*, \mathbf{e}_1^*) \geq u_A(\mathbf{a}_2^*, \mathbf{e}_1^*) \geq u_A(\mathbf{a}_2^*, \mathbf{e}_2^*), \quad (60)$$

and similarly

$$u_A(\mathbf{a}_1^*, \mathbf{e}_1^*) \leq u_A(\mathbf{a}_1^*, \mathbf{e}_2^*) \leq u_A(\mathbf{a}_1^*, \mathbf{e}_2^*). \quad (61)$$

Following the inequalities of (60) and (61) we have that

$$u_A(\mathbf{a}_1^*, \mathbf{e}_1^*) = u_A(\mathbf{a}_2^*, \mathbf{e}_2^*), \quad (62)$$

i.e., the two NEs yield the same utility.